ORNL/TM-6319

DRW - 11

MASTER

Continuous Tokamaks

Y-K. M. Peng

OAK RIDGE NATIONAL LABORATORY
OPERATED BY UNION CARBIDE CORPORATION · FOR THE DEPARTMENT OF ENERGY

ORNL/TM-6319
Dist. Category UC-20a, d, and g

Contract No. W-7405-eng-26

FUSION ENERGY DIVISION

CONTINUOUS TOKAMAKS

Y-K. M. Peng

Date Published - April, 1978

NOTICE This document contains information of a preliminary nature. It is subject to revision or correction and therefore does not represent a final report.

Prepared by the
OAK RIDGE NATIONAL LABORATORY
Oak Ridge, Tennessee 37830
operated by
UNION CARBIDE CORPORATION
for the
DEPARTMENT OF ENERGY

REA

CONTENTS

ABSTRACT

We propose a tokamak configuration that permits the rapid replacement of a plasma discharge in a "burn" chamber by another one in a time scale much shorter than the elementary thermal time constant of the chamber first wall. With respect to the chamber, the effective duty cycle factor can thus be made arbitrarily close to unity minimizing the cyclic thermal stress in the first wall. At least one plasma discharge always exists in the new tokamak configuration, hence, a continuous tokamak. By incorporating adiabatic toroidal compression, configurations of continuous tokamak compressors are introduced. To operate continuous tokamaks, it is necessary to introduce the concept of mixed poloidal field coils, which spatially groups all the poloidal field coils into three sets, all contributing simultaneously to inducing the plasma current and maintaining the proper plasma shape and position. Preliminary numerical calculations of axisymmetric MHD equilibria in continuous tokamaks indicate the feasibility of their continued plasma operation. Advanced concepts of continuous tokamaks to reduce the topological complexity and to allow the burn plasma aspect ratio to decrease for increased beta are then suggested. Comparisons with conventional tokamaks are made in the light of reactor applications, indicating several potential advantages of some advanced continuous tokamaks that require comparable toroidal magnetic field energy to produce comparable fusion power.

1. INTRODUCTION

It is generally expected that scientific feasibility of magnetic fusion energy will be demonstrated in the early 1980's through several large tokamak experiments such as TFTR, Doublet III, and JET. Recent conceptual design studies of tokamak power reactors [1], however, have revealed a number of potentially serious problems that can limit the economic viability of pure tokamak fusion power [2]. Among these problems are (1) the limited lifetime due to fatigue of blanket first wall under cyclic power load and thermal stress [3] and (2) the complexity of interwoven coils and plasma and neutron containment topologies [1]. The former problem tends to limit the time of continued reactor operation before blanket failure, while the latter problem implies extended down-time for blanket repair and maintenance. The combined impact of these two difficulties is expected to significantly constrain the availability of a tokamak reactor and hence increase the overall cost of its power production.

The property of materials for blanket first wall under intense neutron radiation and cycled thermal stress is presently not well understood. Using stainless steel, the first wall thermal stress is anticipated [1,3] to be above the yield stress in tokamak reactors of acceptable thermal efficiency. With such a stress alone, a stainless steel first wall is expected to fail around 10^4 cycles. A discharge pulse length of >60 min would permit continued operation of a tokamak reactor for roughly two years only. This limited time of continued operation is expected

to result in serious economic penalties. There is thus a strong incentive to find ways to operate tokamaks in a steady-state fashion.

Present-day tokamaks are pulsed because the plasma confining current needs to be driven by a toroidally directed electric field induced by a transformer with a limited current capability. Thus, several recent theoretical investigations have explored the possibility of maintaining the plasma current through noninductive processes, e.g., by supplying a net toroidal momentum to the electrons or ions. This process through injections of high and low energy neutral beams was discussed by Ohkawa [4]. The treatment of this beam-driven current as the "seed" current in the presence of a diffusion-driven "bootstrap" current was proposed and analyzed by Bickerton, Connor, and Taylor [5], Sigmar [6], and Sigmar and Rutherford [7]. More recently, the possibility of replacing the beam-driven "seed" current by a net current of the fusion alpha particles is discussed by McNally [8]. Finally, the toroidal electron current may be generated by injecting net momentum waves near the plasma lower hybrid frequency via phased waveguide arrays as proposed by Bers and Fisch [9].

In this paper we propose a different approach in that the inductive process to drive the plasma current remains unaltered. The approach of the continuous tokamak (CT) may be considered as a tokamak analogous to the ion-ring compressor proposed by Fleischmann and Kammash [10] to increase the ion-ring energy from 20 MeV to $\sim$1 GeV. An improved method for obtaining such GeV ion rings was suggested by McNally [11]. Here, we replace each ion ring by a tokamak plasma which is moved from a startup chamber into a burn chamber early in its pulse. The tokamak

plasma is removed to a shutdown chamber near the end of its pulse to allow an already established, new plasma discharge to take its place. This replacement process is to be carried out in a time scale (a small fraction of a second) much shorter than the elementary thermal time constant (approximately a few seconds with certain designs) of the blanket first wall in the burn chamber. As a result, the cycling of thermal stress, which normally is expected to dominate the material stress problems [3], should be significantly reduced. Each plasma pulse still has a finite lifetime in a continuous tokamak. With respect to the burn chamber, however, the duty cycle factor can be made arbitrarily close to unity without requiring long plasma pulses.

The idea of shifting a single plasma discharge in a vacuum chamber has been proposed before in the form of an adiabatic toroidal compressor by Furth and Yoshikawa [12]. Yoshikawa [13] proposed a fusion reactor concept in which the plasma can be heated by compression, brought to a burn chamber where it is maintained for an extended period of time, and then moved to another chamber for shutdown; a new plasma can then be established (e.g., after a few tens of seconds) to repeat the process. In a continuous tokamak, a new plasma is established when the preceding plasma is still in the burn chamber before both are shifted rapidly. Ohyabu et al. [14], recently suggested the concept of a merging tokamak in which another plasma with current in the same direction is formed and shifted to merge with an existing plasma. As will be seen in Section 4, we find it more convenient to alternate the plasma current in the continuous tokamak.

In a continuous tokamak, we no longer have to start up the plasma current in the burn chamber. The poloidal field (PF) coils surrounding the burn chamber can then be simplified; i.e., it is now possible to remove those coils within the plasma loop, leading to advanced concepts of continuous tokamaks. The possibility of significantly reducing the device complexity and the burn plasma aspect ratio in an advanced continuous tokamak will be discussed in this paper.

To show that plasma operations in continuous tokamaks can be carried out, we will first discuss in Section 2 the concept of mixed PF coils. Here we regroup all conventional PF coils to three spatially separate coil sets that simultaneously contribute to inducing the plasma current and to producing the proper vertical and shaping fields. From this coil concept, a simple continuous tokamak will be proposed and examined in Section 3. It will then be generalized to a continuous tokamak compressor (CTC) in Section 4 through inclusion of adiabatic toroidal compression [12]. In these three sections, numerical calculations of axisymmetric magnetohydrodynamic (MHD) equilibria will be carried out to show the feasibility of plasma operation in continuous tokamaks with proper decoupling of flux linkage between coexisting plasmas. Advanced concepts of continuous tokamaks, having no PF coils within the plasma loop in the burn chamber, will be introduced in Section 5. Comparisons with conventional tokamaks in the efficiency of utilizing the toroidal field (TF) energy in reactors will be presented in Section 6. Potential advantages and disadvantages of continuous tokamaks will be discussed in Section 7.

2. MIXED POLOIDAL FIELD COILS

The concept of mixed PF coils may be considered as a generalization of the high β, shell-like coil arrangements [15,16,17] that were recently proposed for use in D-shaped flux conserving tokamaks [18,19]. In those cases the equilibrium field (EF) coils, either interior or exterior to the TF coils, are composed of three groups (inside coils, outside coils, and the D coils in the vicinity of the D-shape tips). The total ampere-turns in these shell-like coils (ΣI_c) are kept to be equal and opposite to the plasma current (I_p). The EF coils thus mimick a conducting shell for reduced power supplies and, in some cases, reduce the pulsed fields at the TF coils. In the case of an air-core tokamak, shell-like coils do not provide sufficient flux swing to produce and maintain an equal plasma current in the opposite direction. A set of conventional ohmic heating coils was therefore introduced [15,17].

The mixed PF coils simply eliminate these air-core ohmic heating coils (see Fig. 1) and allow $|\Sigma I_c|$ in the EF coils to exceed $|I_p|$. This increased coil current is expected to induce and maintain I_p despite imperfect flux linkage to the plasma and the plasma resistivity. As a result, the three coil sets now contribute to vertical field, shaping field, and flux swing, simultaneously. In Fig. 1, we have further constrained the coils to two concentric cylindrical surfaces so that the plasma could be shifted in the direction parallel to the tokamak major axis.

The mixed PF coils can maintain the proper plasma position, shape, and current, as demonstrated by the MHD equilibria shown in Fig. 2.

Here, coil currents are adjusted so that ΣI_c equals $-1.5\ I_p$, $-2\ I_p$, and $-2.5\ I_p$. As expected, the changes in coil currents among these cases follow a fixed distribution which may be considered as the ohmic heating component, superimposed on an EF component. Variations in the EF component will result in changes in the plasma shape. These particular choices of ΣI_c, as an example, imply that $I_c = I_p = 0$ before plasma startup. Thus one could assume that when $\Sigma I_c = -2\ I_p$ the equilibrium is established, fully accounting for the resistive loss of flux swing during startup. The remaining increase in ΣI_c then sustains the plasma in the constant-current phase of the pulse. It is therefore clear that, in principle, other initial values of ΣI_c should also be acceptable. The choice of its value probably depends more on practical considerations (see Sections 5 and 6).

3. SIMPLE CONTINUOUS TOKAMAKS

We can now extend the mixed PF coils to those of a simple continuous tokamak in two steps. First, the coil arrangement and the plasma chamber in Fig. 1 are extended in the z-direction. Secondly, instead of relying on distribution of coils in different coil sets, we switch to distribution of current in regularly spaced coils (see Fig. 3).

In doing so, we gain the freedom of shifting the plasma in the z-direction with a small radial field B_R and a concomitant shift of the current distribution in coils. In Fig. 3, a plasma can be started up to full current near the top of the chamber and shifted to the middle section of the chamber (the burn chamber) early in its constant-current phase. When the limits in coil currents surrounding the burn chamber

are nearly reached, or when the plasma confinement deteriorates for some reason, the plasma can be shifted again to the bottom section of the chamber for shutdown. A single plasma pulse now goes through five phases: startup, intake, burn, exhaust, and shutdown.

The operation of a simple continuous tokamak, as shown in Fig. 3, then consists of starting another plasma (plasma C) near the end of the burn phase of the preceding plasma (plasma B) and (maybe) after the shutdown of the plasma preceding both (plasma A). Plasmas B and C are then shifted simultaneously to the burn and shutdown chambers, respectively. A plasma is absent from the burn chamber only during the time of plasma intake and exhaust. By shifting the plasmas swiftly [in a fraction of a second, a time scale much shorter than the plasma energy confinement time (approximately seconds) but much longer than the MHD time ($\sim$10 μsec)] in and out of the burn chamber, the effective duty cycle factor in a continuous tokamak can, in principle, be made arbitrarily close to unity.

To verify that this process can be carried out, it is necessary to compute, for example, coexisting MHD equilibria for plasmas B and C before the plasma intake and exhaust take place. Also, it is necessary to show that the flux linkage by the two plasmas can be decoupled, so that the startup of one plasma does not influence the current in the other.

The externally produced poloidal flux (ψ_{ext}) that each plasma sees can be decomposed into:

$$\psi_{ext} = \psi_c + \bar{\psi}_c + \psi_p \qquad (1)$$

where ψ_c represents the flux due to currents in local coils, and $\bar{\psi}_c$ and ψ_p represent the flux due to the companion coil and plasma currents, respectively. The desirable ψ_{ext} is known for the given plasma and can be produced by the mixed PF coil currents used in Fig. 2. We have from Eq. (1),

$$\Delta\psi_c = \psi_c - \psi_{ext} = -\bar{\psi}_c - \psi_p \tag{2}$$

which represents the flux that needs to be produced by additional currents (ΔI_i^c) in the local coils to cancel the flux produced by the currents in the companion plasma and coils.

The cancelling currents (ΔI_i^c) for coils near plasmas B and C can be determined iteratively, beginning with the coil currents (I_i^o) for the plasma when each plasma is standing alone. This process can be depicted by the flow chart of Fig. 4. In each step, $[\Delta I_i^c(B)]$ is determined by a simple minimum-squared deviation fit [20] to the flux produced by $[I_i^o(C)]$, $[\Delta I_i^c(C)]$, and $[I_{ij}^p(C)]$, and vice versa. When this process has converged (to $\lesssim$2% squared deviation), the total external flux ψ_{ext} is then used in recomputing both equilibria B and C.

Examples of the stand alone and the continuous tokamak equilibria are shown in Fig. 5, with the corresponding coil currents listed in Table I. Corresponding to Fig. 3, plasma B is at a distance $z_s = 6a$ (a being the plasma minor radius on the midplane) below plasma C. Plasma B is D-shaped with $\bar{\beta} = 5.3\%$ and elongation $\sigma \cong 1.5$, while plasma C is nearly circular with $\bar{\beta} = 1.1\%$ and $\sigma \cong 1.2$. Both equilibria B and C have safety factors $q_o \cong 1.0$, $q_a \cong 3.5$, aspect ratio $A = 4$, and modestly peaked current and pressure profiles [19]. It is seen from Fig. 5 that

the proper shape and position for both plasmas can be maintained in a simple continuous tokamak.

It should be pointed out here that Table I indicates an oscillatory distribution of (ΔI_i^c). This oscillation is apparently due to the fact that the current in each coil shown in Fig. 1 is allowed to vary for the best cancellation of flux $\Delta\psi_c$. The situation is similar to what Lackner [21] has observed in determining the coil current distribution that best reproduces a given plasma shape. More elaborate approaches [21] should result in smooth (ΔI_i^c).

Table I also indicates that the plasma current is assumed to alternate between succeeding plasmas in a continuous tokamak. This is advisable in order to decouple the flux swing between the two companion plasmas by channeling the plasma-linked flux through the space between plasmas B and C. This situation can be reflected by the relatively coarse flux plot (see Fig. 6) produced by all current sources in the continuous tokamak. However, we have not ruled out the possibility of operating a continuous tokamak with the plasma currents in the same direction under certain conditions.

4. CONTINUOUS TOKAMAK COMPRESSOR

It is rather straightforward to modify the simple continuous tokamak into the continuous tokamak compressor by incorporating adiabatic toroidal compression [12]. An artist's depiction of it is given in Fig. 7, which assumes symmetry with respect to the burn chamber and shows that each plasma still goes through five phases. The intake and

exhaust phases are now combined with compression and decompression, respectively.

MHD equilibria calculations for this case are carried out in a fashion similar to the previous case. The results shown in Figs 8 and 9 and Table II assume a compression ratio of 1.6 to result in a plasma minor radius of $a' = 0.79a$ for plasma B. The coils used for plasma B are arranged in a fashion similar to Fig. 1, except with a plasma major radius of $R_o = 2.5a$, coil major radii of $R = 1.3a$ and $3.7a$, and equally spaced coils within $|z| \leq 1.8a$. For convenience, the coils for plasma C are identical to those shown in Fig. 1. The use of a more realistic coil arrangement consistent with Fig. 7 for plasma C is not expected to introduce problems in computing MHD equilibria, for plasma C is low β and nearly circular. The results of Figs 8 and 9 show that proper plasma position and shape can also be maintained in a continuous tokamak compressor with proper decoupling of the plasma-linked fluxes.

5. ADVANCED CONCEPTS OF CONTINUOUS TOKAMAKS

As noted in Section 2, the net ampere-turns (ΣI_c) in the PF coils can be arbitrary as long as the change in ΣI_c during a discharge pulse is sufficient in inducing and maintaining the plasma current. We can choose startup values of ΣI_c so that the currents in the "inside" coils are nearly zero during the burn phase. The induced toroidal electric field in this phase is small, and according to the results of Fig. 2, the required current change in the inside coils is relatively mild. It is therefore possible to maintain the plasma current by current changes

in the D coils (or their equivalent) and the outside coils around the burn chamber and eliminate the inside coils.

The elimination of the inside PF coils represents a significant step toward reducing the topological complexity of tokamaks; they are called advanced continuous tokamaks. A possible example is depicted in Fig. 10. In this figure we have speculated on the possibility of replacing the solid conductors (copper or superconducting) at the central legs of the TF coils by gaseous conductors or electron beams. The aspect ratio of the compressed plasma can then be decreased toward unity, and the plasma beta values as limited by ideal MHD instabilities [22] can be high.

Axisymmetric MHD equilibria with the aspect ratio equal to unity have been calculated by Shafranov [23], Morikawa [24], Morikawa and Rebhan [24], and Yeh and Morikawa [24]. Experiments with such plasmas produced by a rotating relativistic electron beam have been carried out recently by Sethian et al. [25]. Also, Koloc [26] has proposed a method to produce a similar plasma configuration through applications of moderate mechanical pressure. With the exception of having a toroidal field external to the plasma, the poloidal flux configuration of the compressed plasma depicted in Fig. 10 is expected to be similar to the field reversed mirror [27]. The stability of this type of plasma has lately been studied by Sudan and Rosenbluth [28] and by Bussac, Furth, and Rosenbluth [29]. Various particle beams are suggested to maintain the plasma current in these cases. The advanced continuous tokamak offers a different method to produce and maintain small aspect ratio plasmas in a continuous fashion.

6. UTILIZATION OF TOROIDAL FIELD ENERGY

A disadvantage with the continuous tokamak is its apparent ineffective use of TF energy when compared with a conventional tokamak. To quantify the potential limitation, it is convenient to use the simplified geometries shown in Fig. 11. The toroidal magnetic field energy that is contained within the coil bore (E_{BC}) and the plasma (E_{BP}) are roughly given by, respectively,

$$E_{BC} = \frac{\pi H_c}{\mu_0} (B_c R_{c1})^2 \ln\left(\frac{R_{c2}}{R_{c1}}\right) \tag{3}$$

$$E_{BP} = \frac{\pi H_p}{\mu_0} (B_c R_{c1})^2 \ln\left(\frac{R_{p2}}{R_{p1}}\right) \tag{4}$$

where $BR = B_c R_{c1}$; we have assumed rectangular cross sections. In a conventional tokamak, we have

$$\left(\frac{E_{BP}}{E_{BC}}\right)_{conv} = \left(\frac{H_p}{H_c}\right) \ln\left(\frac{A+1}{A-1}\right) \Big/ \ln\left(\frac{A+1+\Delta}{A-1-\Delta}\right) \tag{5}$$

where $A = R_0/a$ is the aspect ratio and Δa is the distance between the plasma and the TF coils. In an advanced continuous tokamak [see Fig. 11(b)], we have

$$\left(\frac{E_{BP}}{E_{BC}}\right)_{CT} = \begin{cases} \left(\frac{H_p}{H_c}\right) \ln\left(\frac{A+1}{A-1}\right) \Big/ \ln\left(\frac{AC + C^{1/2} + \Delta}{A-1}\right) & \text{(fixed C)} \\ \left(\frac{H_p}{H_c}\right) \ln\left(\frac{A+1}{A-1}\right) \Big/ \ln\left(\frac{4 + (2/\sqrt{A}) + \Delta}{A-1}\right) & \text{(fixed } R_{00} = 4a\text{)} \end{cases} \tag{6}$$

where C ($\geq$1) is the compression ratio, R_{00} is the plasma major radius before compression and Δa is the distance between the startup plasma and the TF coils. By comparing Eqs (5) and (6), it is seen that the conventional tokamak has a relatively large value of H_p/H_c, but loses somewhat by a relatively large A.

As a typical example, for Eq. 5 we choose $H_p/H_c = 0.5$, $A = 4$, and $\Delta = 1$, giving $(E_{BP}/E_{BC})_{conv} = 0.23$. For Eq. (6) we assume $H_p/H_c = 1/7$ to plot the dependence of the ratio $[E_{BP}/E_{BC})_{CT}/(E_{BP}/E_{BC})_{conv}]$ on A in Fig. 12. It is seen that this ratio can be between 0.36 and 0.41 if R_{00} is fixed. We shall choose this case in the following discussion.

The effectiveness of utilizing the toroidal field also depends on the plasma $\bar{\beta}$ values, which in turn is related to the fusion power and wall loading in a reactor. For a given first wall material, the wall loading determines the time of continued operation before repair. To correlate these parameters, we use the following simplified formula based on Fig. 11:

$$A_{CT} = 2\pi(R_{p2}H_p + R_{p2}^2 - R_{c1}^2) \tag{7}$$

$$A_{conv} = 2\pi[H_p(R_{p1} + R_{p2}) + R_{p2}^2 - R_{p1}^2] \tag{8}$$

$$V_p = \pi H_p(R_{p2}^2 - R_{p1}^2) \tag{9}$$

where A_{CT} and A_{conv} represent the first wall areas and V_p represents the plasma volume. We further assume that $\bar{\beta}$ is limited by the ideal MHD instability [22]. For a fixed q value, we assume

$$\bar{\beta}_c = \beta_0/A \tag{10}$$

where β_0 depends on the plasma shape and profiles. With an average plasma temperature of 10 keV, the fusion power density (p_{DT}) and plasma density (n) can be approximated by

$$p_{DT} = 0.77\ n^2 \quad (MW/m^3\ ,\ 10^{20}\ m^{-3}) \tag{11}$$

$$n = 1.25\bar{\beta}\ B^2 \quad (10^{20}\ m^{-3}\ ,\ \text{tesla}) \tag{12}$$

Using Eqs (5)-(12), we have for conventional tokamaks the following expressions for E_{BC}, fusion power (P_{DT}), and wall loading (W_L):

$$(E_{BC})_{conv} = \frac{1}{\mu_0}\,\pi a^2 H_c B_c^2 (A - 1 - \Delta)^2\ \ell n\left(\frac{A + 1 + \Delta}{A - 1 - \Delta}\right) \tag{13}$$

$$(P_{DT})_{conv} = 4.8\pi a^2 H_p \beta_0^2\,\frac{B_c^4}{A}\left(\frac{A - 1 - \Delta}{A}\right)^4 \tag{14}$$

$$(W_L)_{conv} = \frac{1.2aH_p}{(H_p + 2a)}\,\beta_0^2\,\frac{B_c^4}{A^2}\left(\frac{A - 1 - \Delta}{A}\right)^4 \tag{15}$$

For advanced continuous tokamaks, we have

$$(E_{BC})_{CT} = \frac{1}{\mu_0}\,\pi a^2 H_c B_c^2 (A - 1)\ \ell n\left(\frac{4 + (2/\sqrt{A}) + \Delta}{A - 1}\right) \tag{16}$$

$$(P_{DT})_{CT} = 4.8\pi a^2 H_p B_0^2\,\frac{B_c^4}{A}\left(\frac{A - 1}{A}\right)^4 \tag{17}$$

$$(W_L)_{CT} = 2.4aH_p\beta_0^2\,\frac{B_c^4}{A[H_p(A + 1) + 2Aa]}\left(\frac{A - 1}{A}\right)^4 \tag{18}$$

It is of interest to examine the ratios of wall area, B_c, E_{BC}, P_{DT}, and W_L ($\bar{A}_{CT}$, $\bar{B}_c$, $\bar{E}_{BC}$, $\bar{P}_{DT}$, and $\bar{W}_L$, respectively) between the continuous tokamak and the conventional tokamak. For convenience, we again assume that A = 4 for the conventional tokamak, that both tokamaks have identical Δ, a, and H_p, and that $(H_c)_{CT} = 3.5\ (H_c)_{conv}$. Note that, if we further assume that $B_c = 10$ T, $\beta_0 = 0.28$, $H_p = 3.2$ m, and a = 1 m for the conventional tokamak, we would obtain from Eq. (8) and Eqs (13)-(15),

$$P_{DT} = 600 \text{ MW}, \qquad A_{conv} = 260 \text{ m}^2$$

$$W_L = 2.3 \text{ MW/m}^2, \qquad E_{BC} = 7.0 \text{ GJ} \tag{19}$$

We can now determine the ratios given the same P_{DT} or W_L for the continuous tokamak. For the same P_{DT}, we obtain from Eqs (7) and (8) and Eqs (13)-(18),

$$\bar{A}_{CT} = [\sigma(A + 1) + 2A]/8(1 + \sigma) \tag{20}$$

$$\bar{B}_c = \frac{A^{1/4}}{2\sqrt{2}} \left(\frac{A}{A - 1}\right) \tag{21}$$

$$\bar{E}_{BC} = \frac{7}{8 \ln 3} \bar{B}_c^2 (A - 1) \ln \left(\frac{4 + 2A^{-1/2} + \Delta}{A - 1}\right) \tag{22}$$

$$\bar{W}_L = 2 \times 16^2 \bar{B}_c^4 \frac{(1 + \sigma)}{A[\sigma(A + 1) + 2A]} \left(\frac{A - 1}{A}\right)^4 \tag{23}$$

where $\sigma = H_p/2a$. Similarly, we have for the same W_L

$$\bar{B}_c = \frac{A^{1/4}}{8^{3/4}} \left[\frac{\sigma(A + 1) + 2A}{1 + \sigma}\right]^{1/4} \left(\frac{A}{A - 1}\right) \tag{24}$$

$$\bar{P}_{DT} = 64\ \bar{B}_c^4\ \frac{1}{A}\left(\frac{A-1}{A}\right)^4 \qquad (25)$$

with $\bar{A}_{CT}$ and $\bar{W}_L$ given by Eqs (20) and (23). The results of Eqs (20)-(25) are plotted in Figs 13 and 14. It is seen from Fig. 13 that, for the same P_{DT}, $\bar{E}_{BC}$ can be made less than unity if values of $\bar{W}_L$ above 2.4 can be tolerated. This implies a compression ratio above two. The maximum value for $\bar{E}_{BC}$ is somewhat above two with $\bar{W}_L$ around 1.5 when little compression is applied. From Fig. 14, it is seen that for the same W_L, the values of $\bar{E}_{BC}$ and $\bar{P}_{DT}$ can range from 0.3 to 1.7 and from 0.3 to 0.7, respectively, as the compression ratio varies from 3.3 down to nearly 1.

These estimates show that the penalties in E_{BC} and W_L for the continuous tokamak are up to a factor of ∿2 to 3 above the conventional tokamak. Parameter ranges do exist, however, in which either or both of $\bar{E}_{BC}$ and $\bar{W}_L$ can be made to fall between 0.5 and 1.5. Intuitively, the possibility of high $\bar{\beta}$ (>0.1) with a small aspect ratio (≲2) apparently results in low values of $\bar{E}_{BC}$ for continuous tokamaks. $\bar{E}_{BC}$ can be reduced by a factor of roughly two if time-averaged P_{DT} is used for a conventional tokamak with a duty cycle factor of roughly 0.5.

7. DISCUSSION

In addition to the possibility of minimizing the cyclic thermal stress, continuous tokamak reactors apparently have these potential advantages:

(1) The engineering complexity is expected to be significantly less than that of a conventional tokamak reactor because of the elimination of the inside coils and possibly the part of blanket

and shield that links the burn plasma loop. Further, simplification is expected through the separation of the plasma startup chamber where large penetrations are required for neutral beams, poloidal or bundle divertors [30] and vacuum pumps, from the burn chamber where the blanket is required. Simple estimates show that roughly 25% of the fusion neutrons would go through the intake and exhaust openings to the burn chamber if the height of the chamber is 3 H_p in the z-direction. Additional blankets directly above and below the chamber (see Fig. 10) would reduce this loss. Neutron shielding required for sensitive elements in neutral beam injectors and divertors can be reduced since these are now out of the line of sight of the fusion plasma.

(2) It is well known that adiabatic toroidal compression [12] will significantly reduce the neutral beam power and energy [13,31], the plasma temperature, and density required in the startup plasma immediately before compression.

(3) The plasma burn time in a continuous tokamak, in principle, needs only to be longer than the time required to establish a new startup plasma (e.g., tens of seconds), although a further extended burn time is certainly desirable. Active fueling is still required since the particle confinement time is expected to be a few seconds. Some form of plasma impurity control will similarly be desirable. The continuous tokamak may be considered as providing an option of not having to maintain the quality of each burn plasma for times much longer than tens of seconds in a reactor.

The following potential disadvantages of continuous tokamaks should also be mentioned; these tend to be related to a lack of detailed understanding at the present time.

(1) The plasma shape and position control are expected to be significantly more complicated than in conventional tokamaks. However, the power required for plasma compression is expected to be acceptable.

(2) Pulsed poloidal fields at the TF coils may be significant during plasma startup, intake, and exhaust. It may be necessary to slow down the plasma startup process by programmed auxiliary heating methods with neutral beams [32] and/or upper hybrid waves [33], easing somewhat the plasma control requirements during startup. During intake and exhaust, it may be necessary to have $\Sigma I_c \cong -I_p$.

(3) Gas loading on the burn plasma from startup and shutdown chambers may be difficult to control.

(4) Although E_{BC} can be comparable to the conventional tokamak, the overall size of the continuous tokamak is relatively large.

(5) Without PF coils within the burn plasma loop, the plasma column may be unstable with respect to displacements in the z-direction.

Further studies are needed to better understand the usefulness of continuous tokamaks.

ACKNOWLEDGEMENTS

The author has benefitted much from several discussions with Drs. Don Steiner, T. E. Shannon, W. M. Wells, and P. B. Mohr of the Oak Ridge TNS Program. Several discussions with Drs. R. A. Dory, John Sheffield, D. J. Sigmar, and J. R. McNally, Jr., during this work have also been highly valuable.

Research sponsored by the Office of Fusion Energy (ETM), U.S. Department of Energy under contract W-7505-eng-26 with the Union Carbide Corporation.

REFERENCES

[1] STEINER, D., et al., "ORNL Fusion Power Demonstration Study: Interim Report," Oak Ridge National Laboratory Report ORNL/TM-5813 (1977); STACEY, W.M., Jr., et al., "EPR-77, A Revised Design for Tokamak Experimental Power Reactor," Argonne National Laboratory Report ANL/FPP/TM-77 (1977); BADGER, B., CONN, R.W., KULCINSKI, G.L., et al., "UWMAK-III, A Noncircular Tokamak Power Reactor Design," Electric Power Research Institute Report EPRI-ER-368 (1976); MILLS, R.G., "Some Engineering Problems of Thermonuclear Reactors," Princeton Plasma Physics Laboratory Report MATT-548 (1967); Fusion Engineering Staff, "Conceptual Design Study of a Noncircular Tokamak Demonstration Fusion Power Reactor," General Atomic Report GA-A13992 (1976).

[2] METZ, W.D., Science 193 (1976) 38.

[3] ABDOU, M., HARKNESS, S.D., MAJUMDAR, S., MARONI, V., MISRA, B., CRAMER, R., DAVIS, J., DeFREEZE, D., KUMMER, D., "The Establishment of Alloy Development Goals Important to the Commercialization of Tokamak Based Fusion Reactors," Argonne National Laboratory Report ANL/FPP/TM-99, MDCE-1743 (1977).

[4] OHKAWA, T., Nucl. Fusion 10 (1970) 185.

[5] BICKERTON, R.J., CONNOR, J.W., TAYLOR, J.B., Nature Physical Science 229 (1971) 110.

[6] SIGMAR, D.J., Nucl. Fusion 13 (1973) 17.

[7] SIGMAR, D.J., RUTHERFORD, P.H., Nucl. Fusion 13 (1973) 677.

[8] McNALLY, J.R., Jr., "On the Possibility of a Stable, Steady-State Tokamak Reactor" (to be published).

[9] BERS, A., FISCH, N.J., Proc. 3rd Topical Conf. on Radio Frequency Plasma Heating, Pasadena, CA, 1978 (to be published).

[10] FLEISCHMANN, H.H., KAMMASH, T., Nucl. Fusion 15 (1975) 1143.

[11] McNALLY, J.R., Jr., "Simplified Approach to Attaining a Proton E-layer," Oak Ridge National Laboratory Report ORNL/TM-4965 (1975).

[12] FURTH, H.P., YOSHIKAWA, S., Phys. Fluids 13 (1970) 2593.

[13] YOSHIKAWA, S., "A Possible Fusion Reactor," Princeton Plasma Physics Laboratory Report MATT-1253 (1976).

[14] OHYABU, N., HSIEH, C.L., JENSEN, T.H., "Merging Tokamak," General Atomic Report GA-A14083 (1977).

[15] CALLEN, J.D., CLARKE, J.F., DORY, R.A., HOLMES, J.A., MARCUS, F.B., McALEES, D.G., MOORE, J.R., NELSON, D.B., PENG, Y-K.M., SAYER, R.O., SIGMAR, D.J., STRICKLER, D.J., TSANG, K.T., UCKAN, N.A., "Tokamak Plasma Magnetics," in Plasma Physics and Controlled Nuclear Fusion

Research (Proc. 6th Int. Conf., Berchtesgaden) 2, IAEA, Vienna (1977) 369.

[16] PENG, Y-K.M., DORY, R.A., STRICKLER, D.J., SWAIN, D.W., "Poloidal Fields and Noncircular MHD Equilibria Calculations in ISX-B" (to be published).

[17] PENG, Y-K.M., STRICKLER, D.J., DORY, R.A., "Hybrid Equilibrium Field Coils in the ORNL TNS" (Proc. 7th Symp. on Engineering Problems of Fusion Research, Knoxville, TN) 1 (1977) 186.

[18] CLARKE, J.F., SIGMAR, D.J., Phys. Rev. Lett. 38 (1977) 70.

[19] DORY, R.A., PENG, Y-K.M., Nucl. Fusion 17 (1977) 21.

[20] PENG, Y-K.M., MARCUS, F.B., DORY, R.A., MOORE, J.R., "Magnetic Shielding System in a Tokamak Experimental Power Reactor — Concept and Calculations" (Proc. 6th Symp. on Engineering Problems of Fusion Research, San Diego, CA) 1 (1975) 1114.

[21] LACKNER, K., Comp. Phys. Comm. 12 (1976) 33.

[22] DOBROTT, D., NELSON, D.B., GREENE, J.M., GLASSER, A.H., CHANCE, M.S., FRIEMAN, E.A., Phys. Rev. Lett. 39 (1977) 943.

[23] SHAFRANOV, V.D., in Reviews of Plasma Physics (LEONTOVICH, M.A., Ed., Consultants Bureau Enterprises, Inc., New York) 2 (1966).

[24] MORIKAWA, G.K., Phys. Fluids 12 (1969) 1648; MORIKAWA, G.K., REBHAN, E., Phys. Fluids 13 (1970) 497; YEH, T., MORIKAWA, G.K., Phys. Fluids 14 (1971) 781.

[25] SETHIAN, J.D., GERBER, K.A., SPECTOR, D.N., GOLDENBAUM, G.C., HAMMER, D.A., ROBSON, A.E., Bull. Am. Phys. Soc. 22 (1977) 1155.

[26] KOLOC, P.M., Bull. Am. Phys. Soc. 21 (1976) 1194; 22 (1977) 1152.

[27] BALDWIN, D.E., Comments on Plasma Physics and Controlled Fusion 2 (1977) 173.

[28] SUDAN, R.N., ROSENBLUTH, M.N., Phys. Rev. Lett. 36 (1976) 972.

[29] BUSSAC, M.N., FURTH, H.P., ROSENBLUTH, M.N., private communication.

[30] SHEFFIELD, J., DORY, R.A., "The Ripple Bundle Divertor for Tokamaks," Oak Ridge National Laboratory Report ORNL/TM-6220 (1978).

[31] COHN, D.R., JASSBY, D.L., KREISCHER, K., "Neutral-Beam Requirements for Compression-Boosted Ignited Tokamak Plasmas," Princeton Plasma Physics Laboratory Report PPPL-1405 (1977).

[32] GIRARD, J.P., KHELLADI, M., MARTY, D.A., Nucl. Fusion 13 (1973) 685.

[33] PENG, Y-K.M., BOROWSKI, S.K., "Microwave Start-up of Tokamak Plasmas Near Electron Cyclotron and Upper Hybrid Resonances," submitted to Nucl. Fusion; also Oak Ridge National Laboratory Report ORNL/TM-6112 (1977).

Table I. Currents in coils for plasmas B and C, when they are alone and when they are coexisting in a simple continuous tokamak, corresponding to the equilibria shown in Fig. 5

	Plasma B ($\Sigma I_c = -2.5\ I_p$, $I_p = 9.3$)		Plasma C ($\Sigma I_c = -2\ I_p$, $I_p = -7.6$)	
Coil #	$-I_i^o/I_p$	$-(I_i^o + \Delta I_i^c)/I_p$	$-I_i^o/I_p$	$-(I_i^o + \Delta I_i^c)/I_p$
1	0	-0.259	0	0.643
2	0.330	0.440	0.393	-0.246
3	0	-0.078	0	0.131
4	0.154	0.130	0.089	-0.014
5	0.154	0.111	0.089	0.052
6	0.154	0.122	0.089	0.014
7	0.154	0.098	0.089	0.067
8	0	0.054	0	-0.142
9	0.330	-0.024	0.393	0.592
10	0	0.369	0	-0.429
11	0.204	0.825	0.143	0.016
12	0.204	-0.169	0.143	0.248
13	0	0.107	0	-0.034
14	0.204	0.184	0.143	0.159
15	0	0.010	0	-0.004
16	0	-0.004	0	0.016
17	0.204	0.214	0.143	0.115
18	0	-0.023	0	0.163
19	0.204	0.279	0.143	-0.418
20	0.204	0.111	0.143	1.071

Table II. Currents in coils for plasmas B and C, when they are alone and when they are coexisting in a continuous tokamak compressor, corresponding to the equilibria shown in Fig. 8

	Plasma B ($\Sigma I_c = -3\ I_p$, $I_p = 16$)		Plasma C ($\Sigma I_c = -2\ I_p$, $I_p = -7.6$)	
Coil #	$-I_i^o/I_p$	$-(I_i^o + \Delta I_i^c)/I_p$	$-I_i^o/I_p$	$-(I_i^o + \Delta I_i^c)/I_p$
1	0	-0.219	0	1.128
2	0.465	0.630	0.393	-0.571
3	0	-0.111	0	0.201
4	0.210	0.225	0.089	-0.027
5	0.210	0.167	0.089	0.054
6	0.210	0.211	0.089	0.012
7	0.210	0.139	0.089	0.071
8	0	0.131	0	-0.158
9	0.465	0.049	0.393	0.614
10	0	0.389	0	-0.445
11	0.205	0.426	0.143	-0.007
12	0.205	0.085	0.143	0.268
13	0	0.038	0	-0.046
14	0.205	0.206	0.143	0.159
15	0	0.006	0	-0.011
16	0	0.004	0	0.015
17	0.205	0.207	0.143	0.097
18	0	0.009	0	0.187
19	0.205	0.196	0.143	-0.492
20	0.205	0.211	0.143	0.952

FIGURE CAPTIONS

Fig. 1. The PF coil arrangement used in the equilibrium calculations. The solid circles indicate the mixed PF coils used in calculating equilibria in a conventional tokamak as shown in Fig. 2. The solid and dashed lines indicate the numerical grid boundaries and the limiters, respectively.

Fig. 2. D-shaped flux surfaces of plasmas with $\bar{\beta} = 5.3\%$, $q_o \cong 1$, $q_a \cong 3.5$, and $A = 4$, maintained by the mixed PF coils. Three groups of coils are used with $I_2 = I_9$ (D coils), $I_4 = I_5 = I_6 = I_7$ (inside coils), and $I_{11} = I_{12} = I_{14} = I_{17} = I_{19} = I_{20}$ (outside coils, see Fig. 1). (a) $\Sigma I_c = -1.5\ I_p$, $I_2 = 0.034\ I_p$, $I_4 = -0.108\ I_p$, $I_{11} = -0.190\ I_p$, (b) $\Sigma I_c = -2.0\ I_p$, $I_2 = -0.148\ I_p$, $I_4 = -0.131\ I_p$, $I_{11} = -0.197\ I_p$, (c) $\Sigma I_c = -2.5\ I_p$, $I_2 = -0.330\ I_p$, $I_4 = -0.154\ I_p$, $I_{11} = -0.204\ I_p$.

Fig. 3. Schematic coil and vacuum vessel configuration in a simple continuous tokamak.

Fig. 4. The iterative process used to determine the cancelling current (ΔI_i^c) needed to nullify the flux produced by the companion plasma current filaments (I_{ij}^p) and coil currents ($I_i^o + \Delta I_i^c$) in a continuous tokamak.

Fig. 5. MHD equilibria for plasmas B and C when they stand alone [(a) and (b)] and when they form a pair [(c) and (d)] in a simple continuous tokamak. The coils and their currents for each equilibrium are shown in Fig. 1 and Table I, respectively.

Fig. 6. Poloidal flux produced by all current sources in a simple continuous tokamak with plasmas B and C of Fig. 5 and Table I.

Fig. 7. Schematic coil and vacuum vessel configuration in a continuous tokamak compressor.

Fig. 8. MHD equilibria for plasmas B and C when they stand alone [(a) and (b)] and when they form a pair [(c) and (d)] in a continuous tokamak compressor. The coils and their currents used for each equilibrium are shown in Fig. 1 and Table II, respectively.

Fig. 9. Poloidal flux produced by all current sources in a continuous tokamak compressor with plasmas B and C of Fig. 8 and Table II.

Fig. 10. Schematic configuration of a possible advanced continuous tokamak reactor.

Fig. 11. Simplified configurations of (a) a conventional tokamak and (b) an advanced continuous tokamak used for comparison.

Fig. 12. The fraction of TF energy occupied by the plasma in an advanced continuous tokamak relative to that in a conventional tokamak.

Fig. 13. The ratios of E_{BC}, W_L, B_c, and A_{CT} between the advanced continuous tokamak and the conventional tokamak with the same P_{DT} as a function of A of the compressed plasma.

Fig. 14. The ratios of E_{BC}, P_{DT}, B_c, and A_{CT} between the advanced continuous tokamak and the conventional tokamak with the same W_L as a function of A of the compressed plasma.

ORNL/DWG/FED 78-205

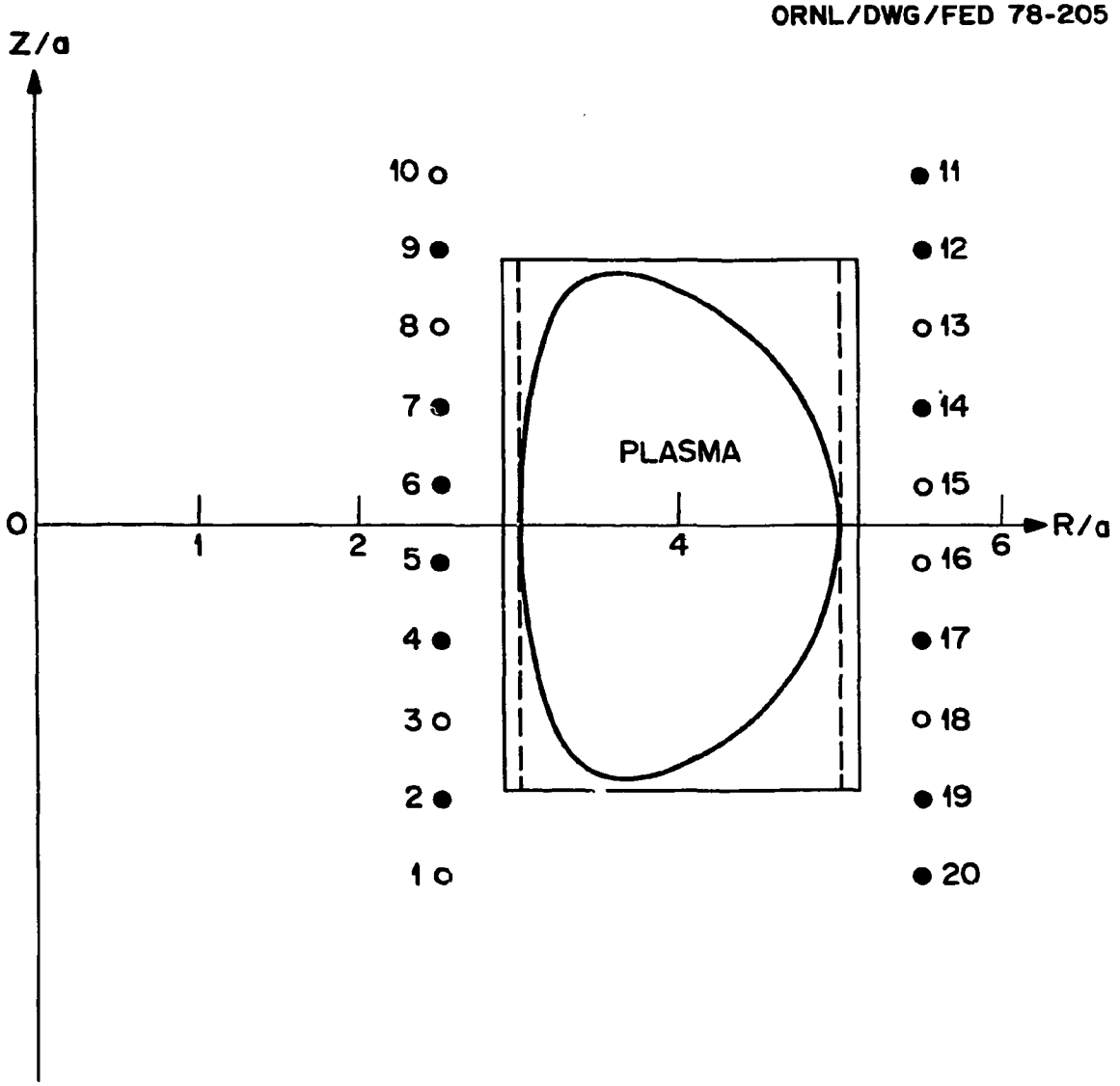

Fig. 1.

BLANK PAGE

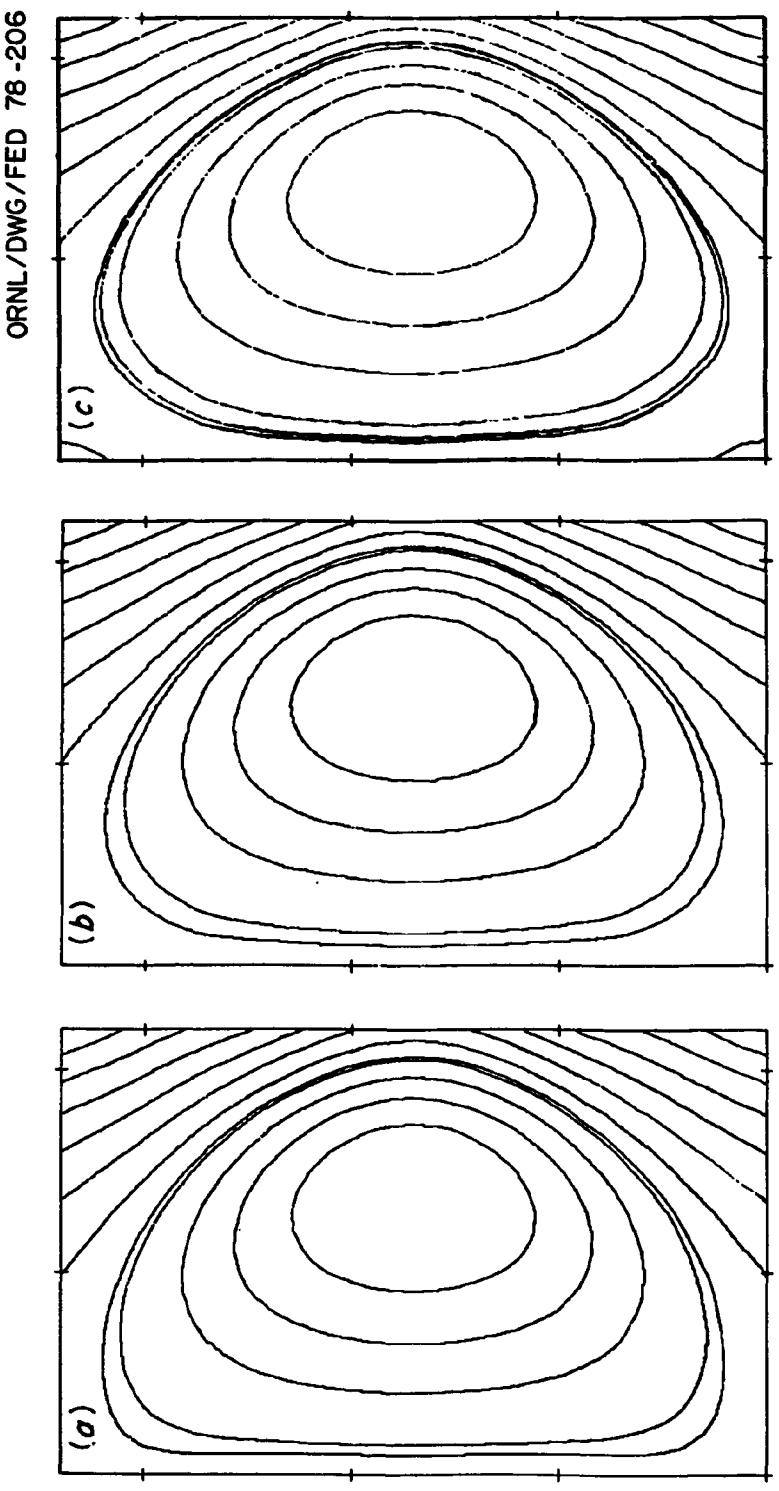

Fig. 2.

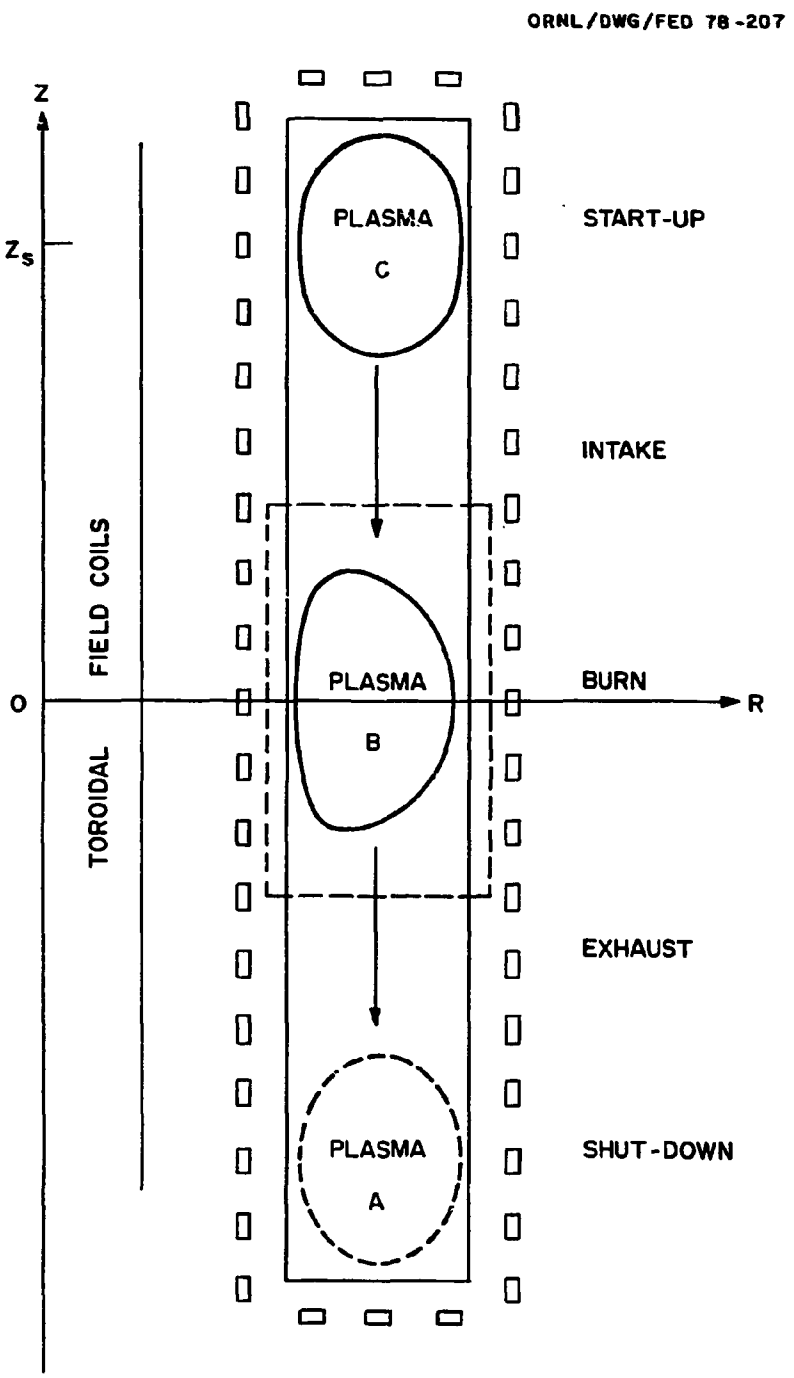
ORNL/DWG/FED 78-207
Z
Z_s
0
R
FIELD COILS
TOROIDAL
PLASMA
C
PLASMA
B
PLASMA
A
START-UP
INTAKE
BURN
EXHAUST
SHUT-DOWN

Fig. 3.

ORNL/DWG/FED-78-208

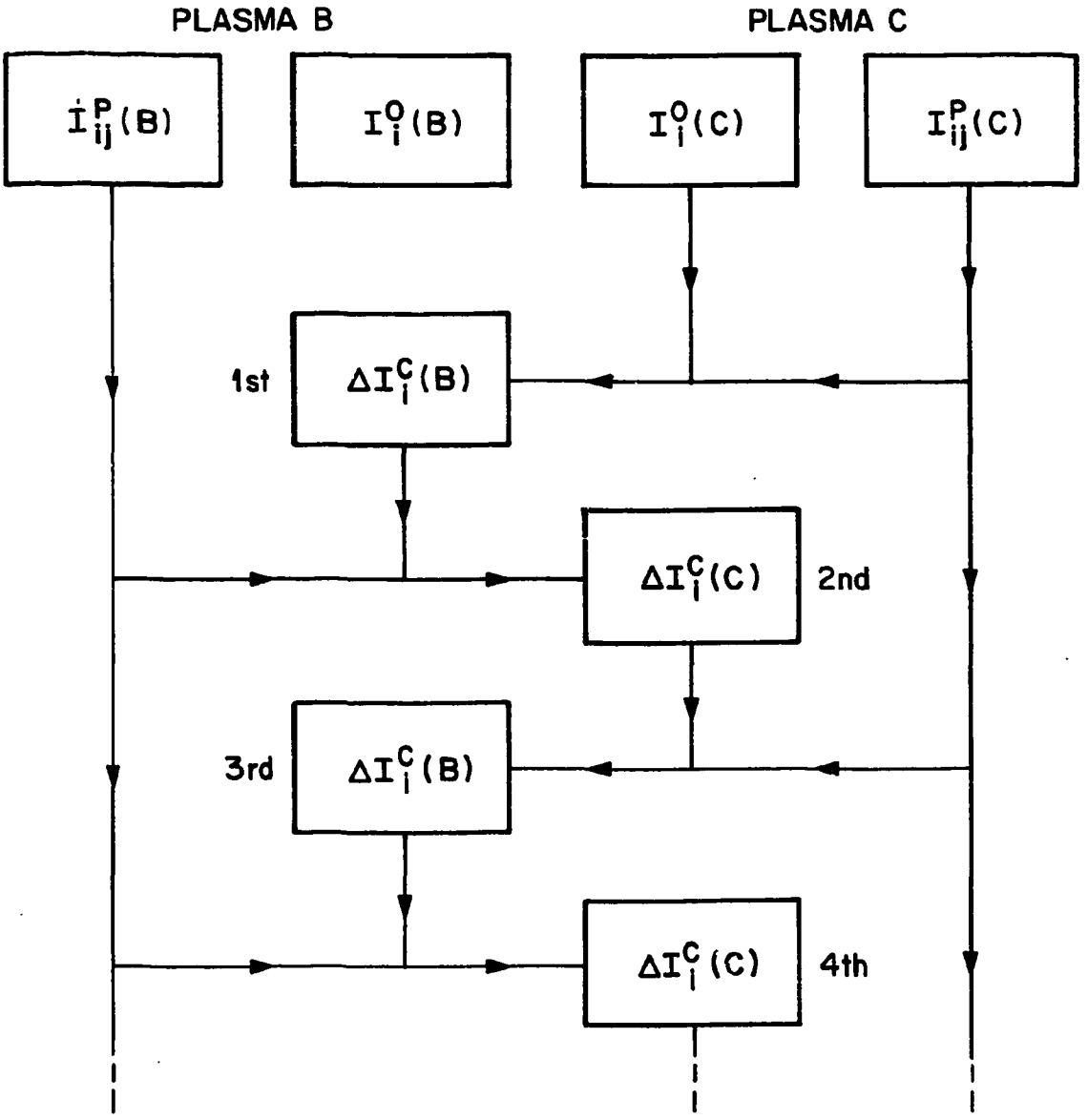

Fig. 4.

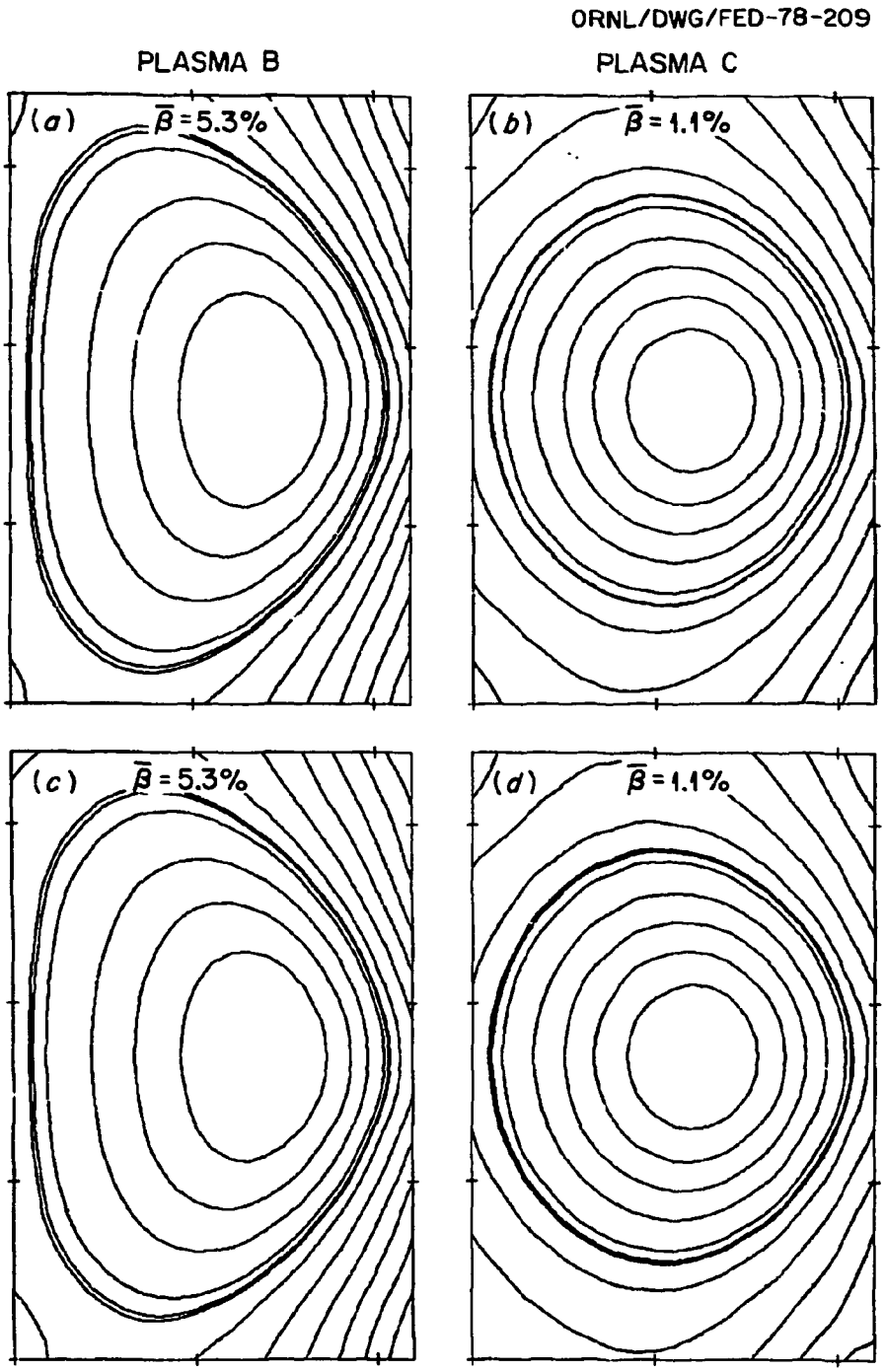
ORNL/DWG/FED-78-209
PLASMA B
PLASMA C
(a)
$\bar{\beta}$ = 5.3%
(b)
$\bar{\beta}$ = 1.1%
(c)
$\bar{\beta}$ = 5.3%
(d)
$\bar{\beta}$ = 1.1%

Fig. 5.

ORNL/DWG/FED-78-210

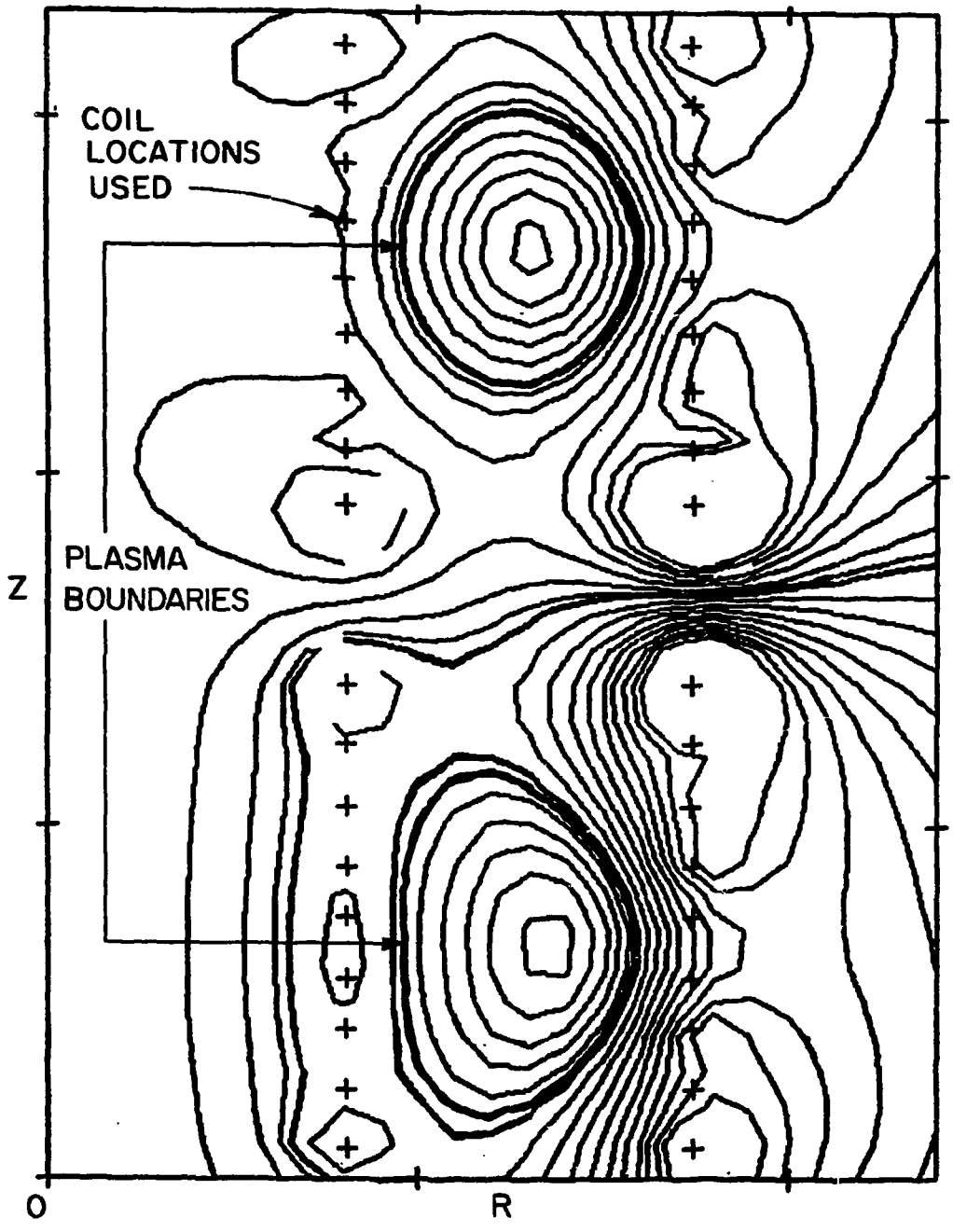

Fig. 6.

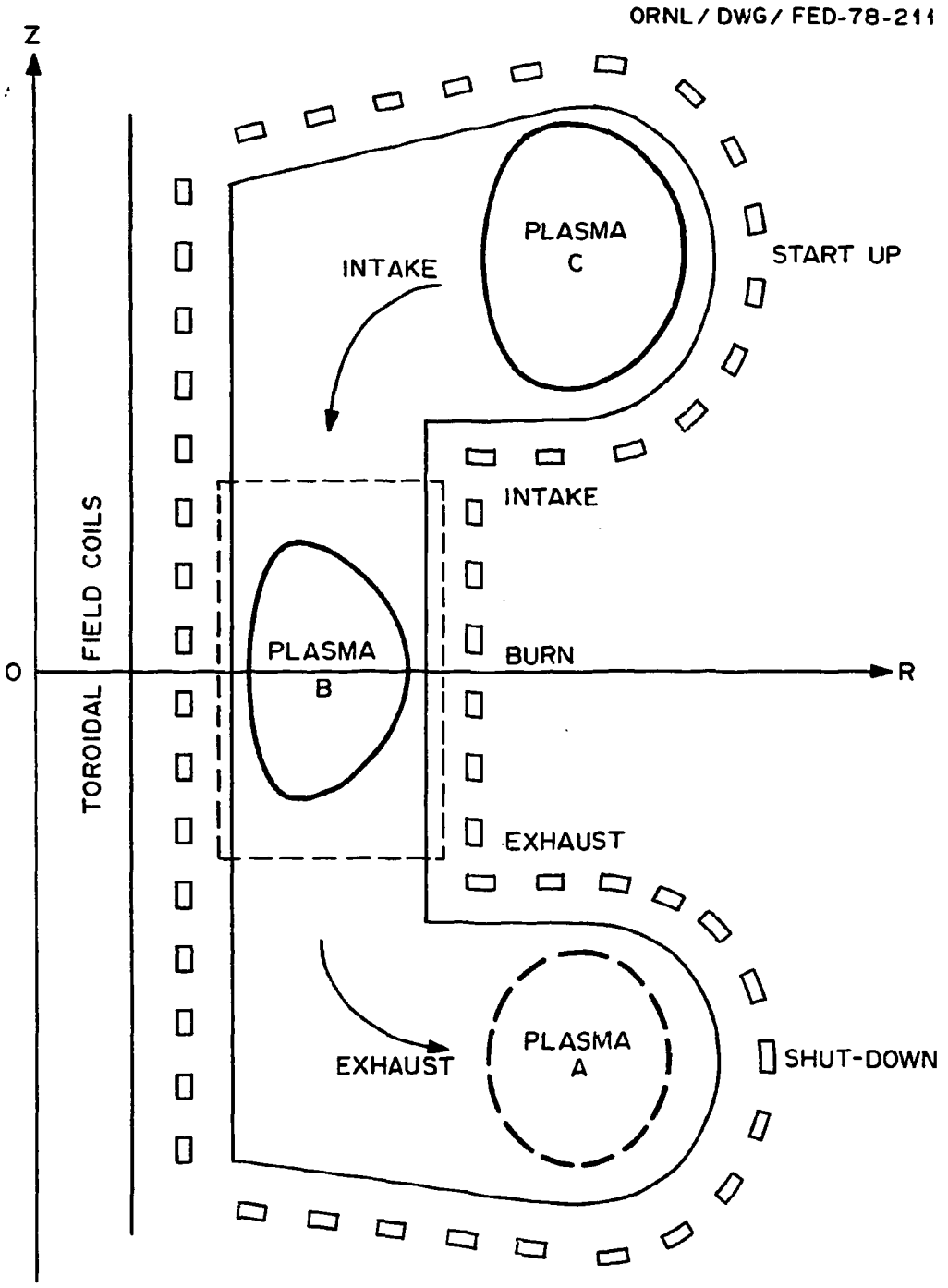
ORNL / DWG / FED-78-211
Z
R
O
TOROIDAL FIELD COILS
PLASMA
C
START UP
INTAKE
INTAKE
PLASMA
B
BURN
EXHAUST
EXHAUST
PLASMA
A
SHUT-DOWN

Fig. 7.

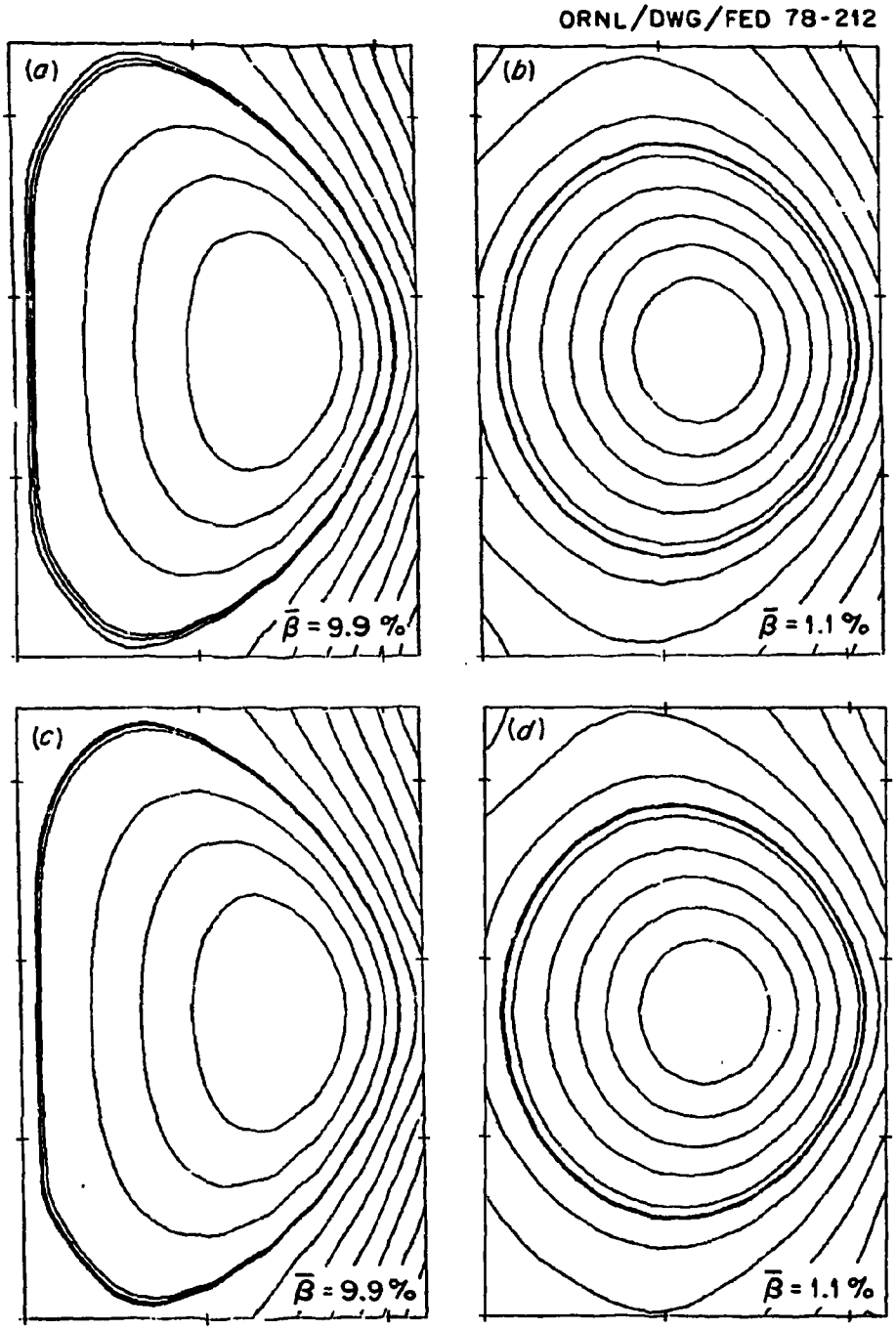
ORNL/DWG/FED 78-212
(a)
$\bar{\beta}$ = 9.9 %
(b)
$\bar{\beta}$ = 1.1 %
(c)
$\bar{\beta}$ = 9.9 %
(d)
$\bar{\beta}$ = 1.1 %

Fig. 8.

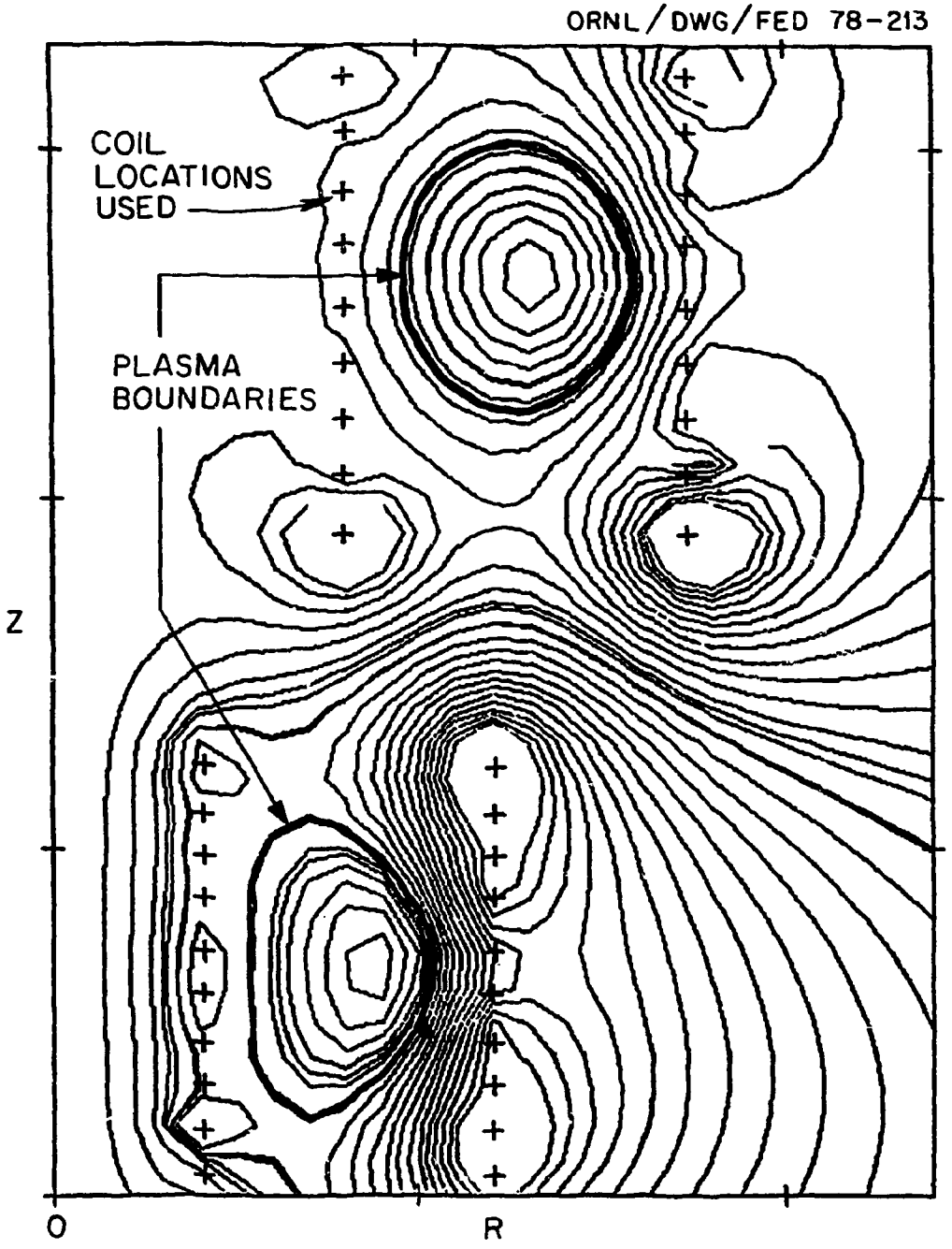
ORNL/DWG/FED 78-213
COIL
LOCATIONS
USED
PLASMA
BOUNDARIES
Z
0
R

Fig. 9.

ORNL/DWG/FED-78-214

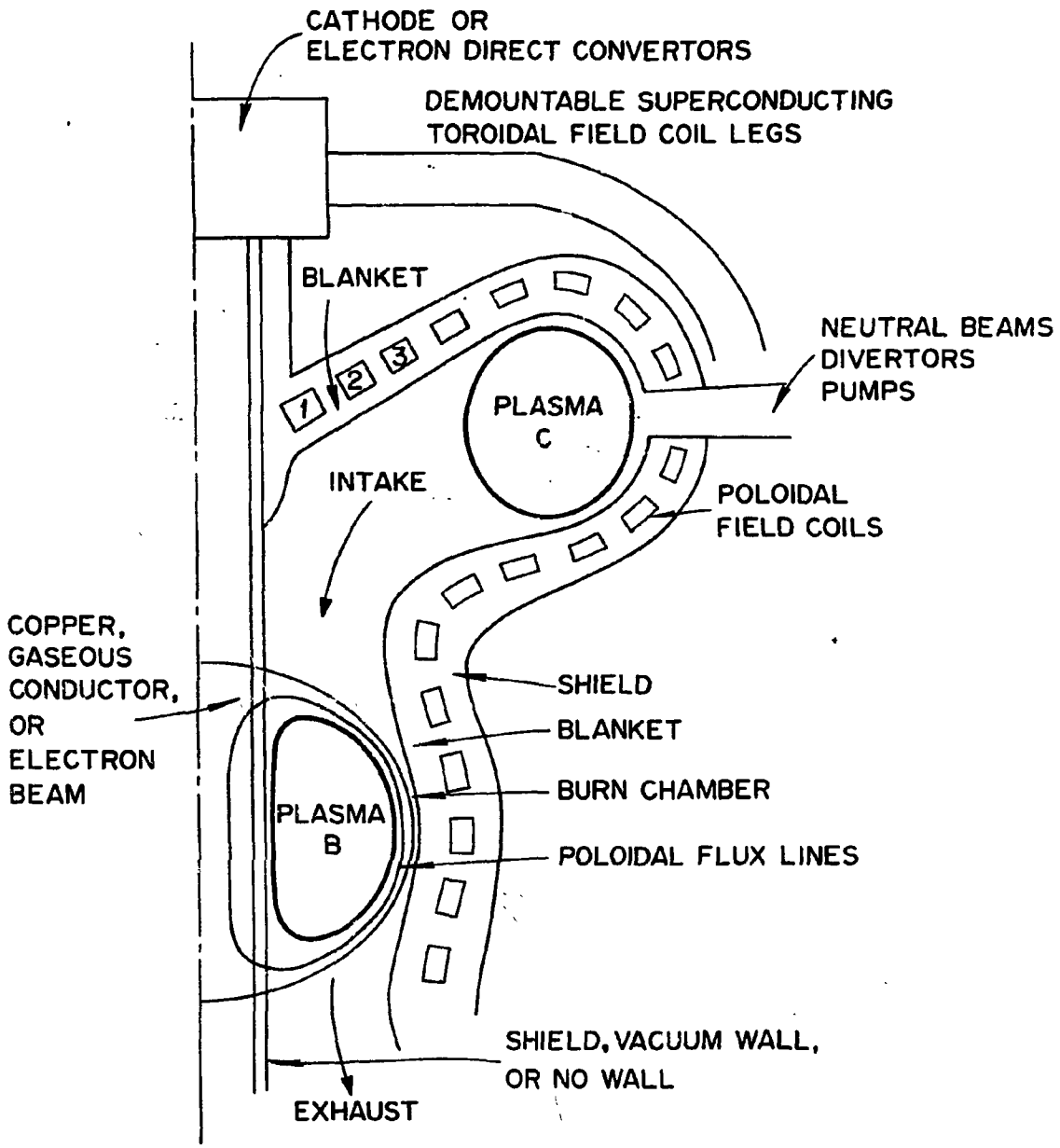

Fig. 10.

ORNL/DWG/FED-78-215

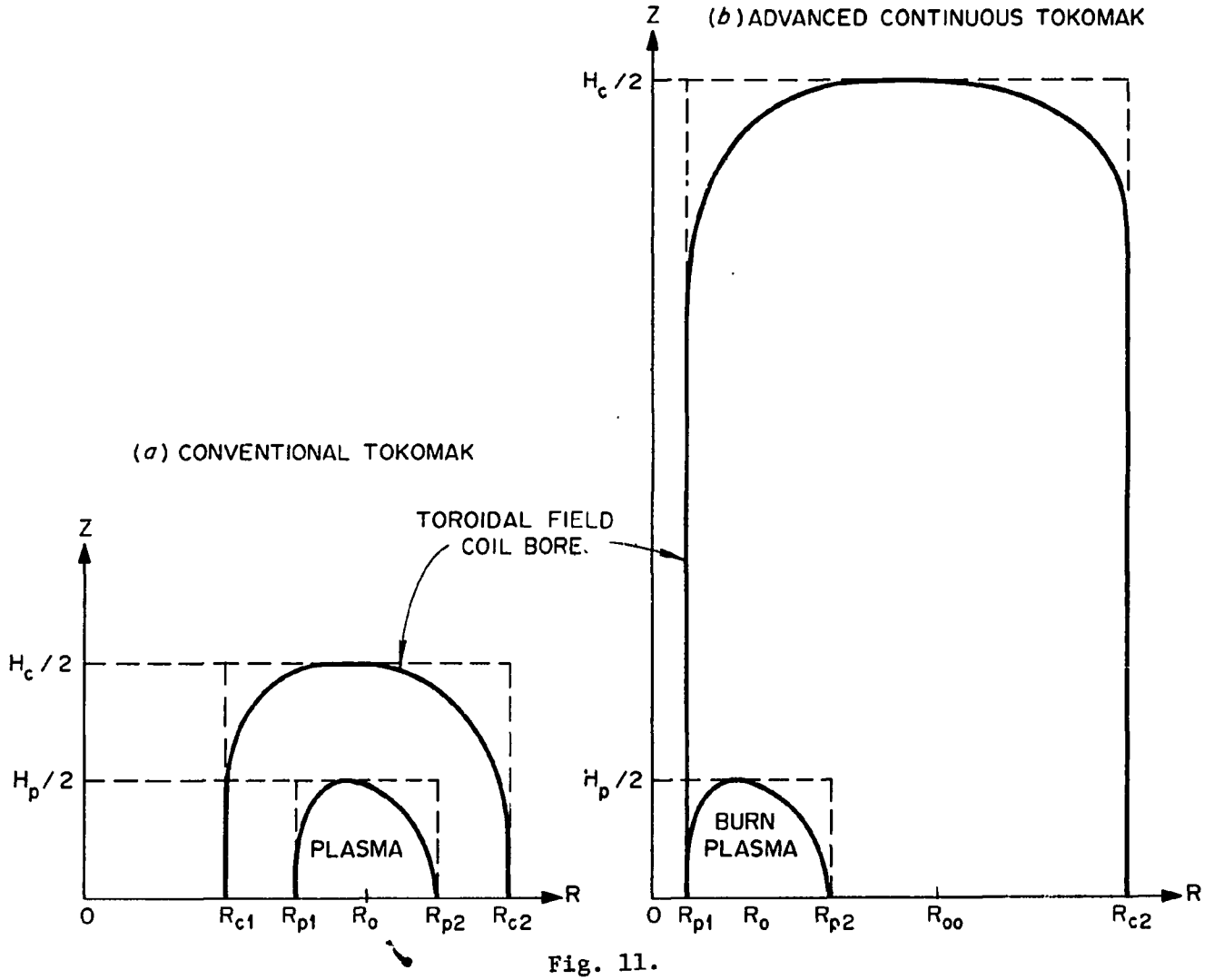

Fig. 11.

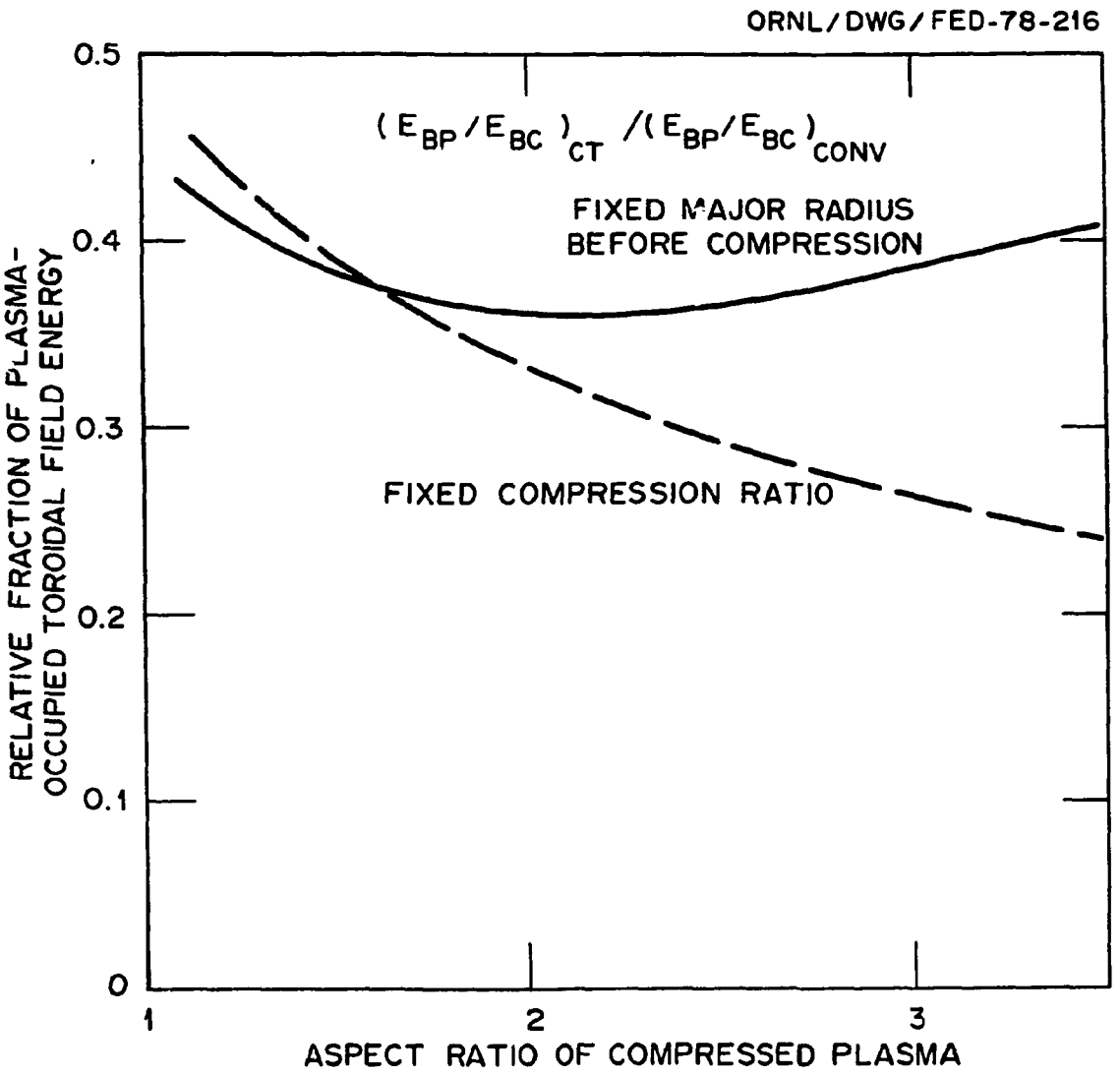
ORNL/DWG/FED-78-216
0.5
0.4
0.3
0.2
0.1
0
RELATIVE FRACTION OF PLASMA-OCCUPIED TOROIDAL FIELD ENERGY
$(E_{BP}/E_{BC})_{CT}/(E_{BP}/E_{BC})_{CONV}$
FIXED MAJOR RADIUS BEFORE COMPRESSION
FIXED COMPRESSION RATIO
1
2
3
ASPECT RATIO OF COMPRESSED PLASMA

Fig. 12.

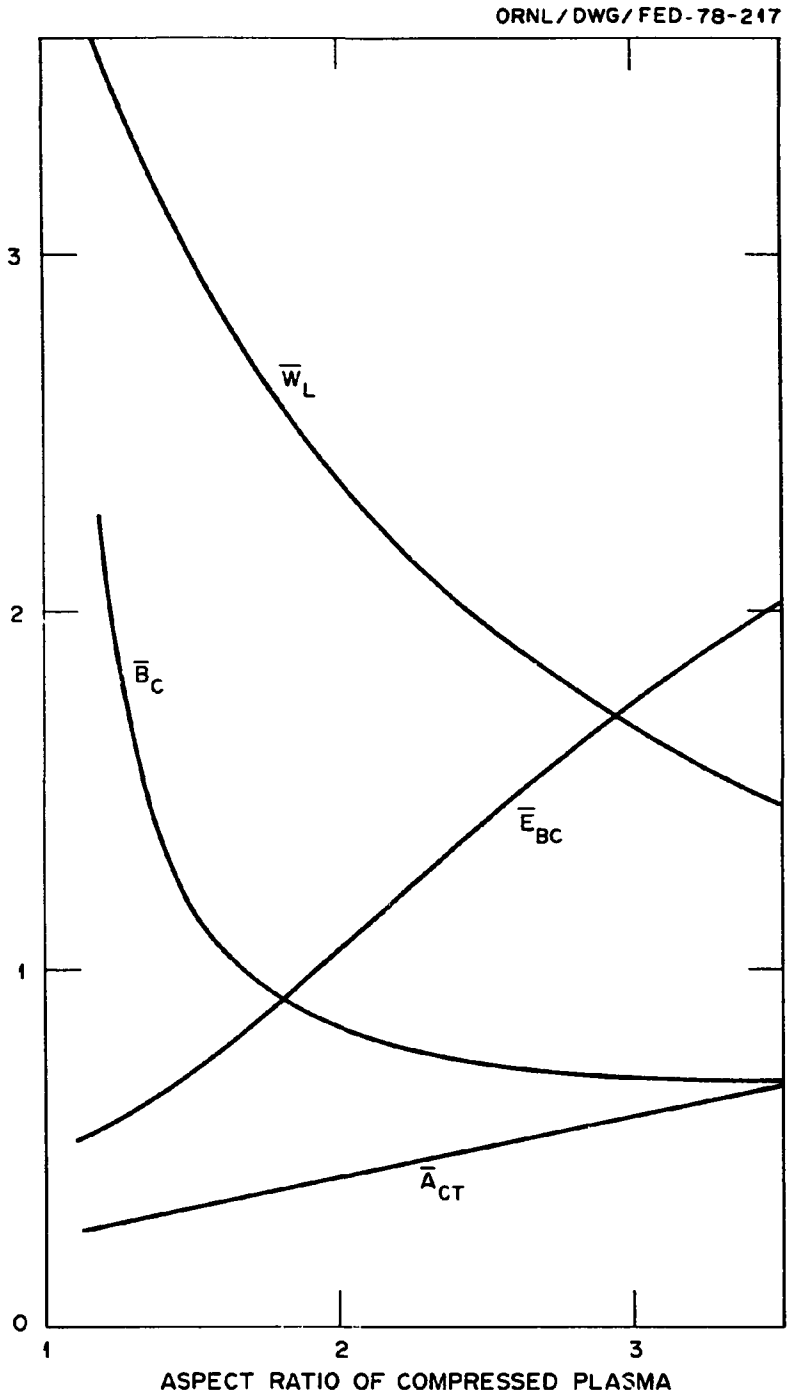
ORNL/DWG/FED-78-217
3
2
1
0
1
2
3
$\overline{W}_L$
$\overline{B}_C$
$\overline{E}_{BC}$
$\overline{A}_{CT}$
ASPECT RATIO OF COMPRESSED PLASMA

Fig. 13.

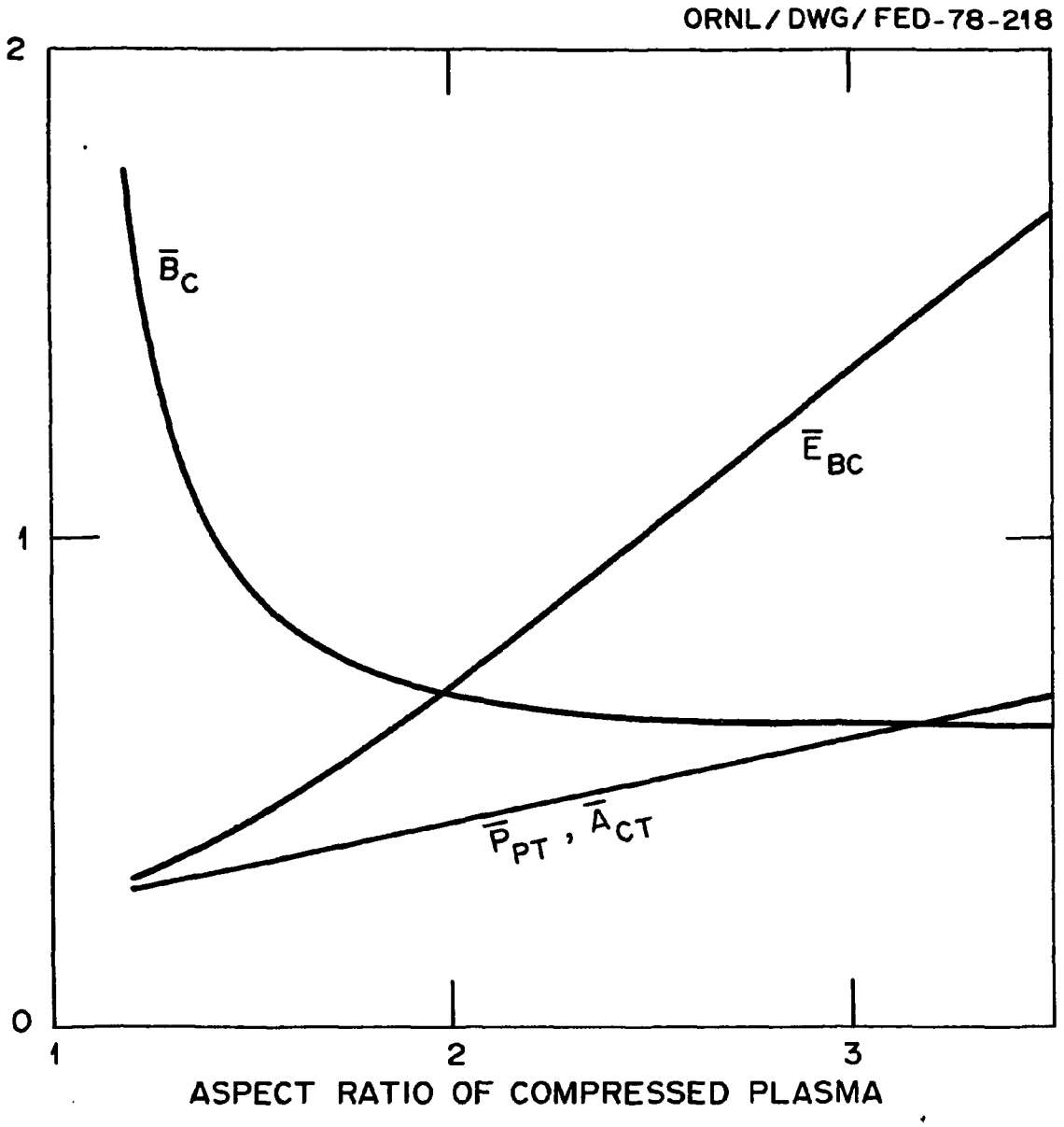
ORNL/DWG/FED-78-218
2
1
0
$\bar{B}_C$
$\bar{E}_{BC}$
$\bar{P}_{PT}$, $\bar{A}_{CT}$
1
2
3
ASPECT RATIO OF COMPRESSED PLASMA

Fig. 14.

ORNL/TM-6319
Dist. Category UC-20a, d, and g

INTERNAL DISTRIBUTION

1. L. A. Berry
2. J. D. Callen
3. R. A. Dandl
4. R. A. Dory
5. G. G. Kelley
6. H. H. Haselton
7. P. N. Haubenreich
8. M. S. Lubell
9. O. B. Morgan
10. H. Postma
11. M. W. Rosenthal
12. J. Sheffield
13. D. Steiner
14-39. Y-K. M. Peng
40-41. Laboratory Records Department
42. Laboratory Records, ORNL-RC
43. Document Reference Section
44-45. Central Research Library
46. Fusion Energy Division Library
47. Fusion Energy Division Communications Center
48. ORNL Patent Office

EXTERNAL DISTRIBUTION

49. Bibliothek, Max-Planck Institute für Plasmaphysik, 8046 Garching bei München, Federal Republic of Germany
50. Bibliothèque, Service du Confinement des Plasmas, C.E.A., B.P. No. 6, 92, Fontenay-aux Roses (Seine), France
51. Lung Cheung, Department of Electronics, University Science Center, The Chinese University of Hong Kong, Shatin, N.T., Hong Kong
52. J. F. Clarke, Office of Fusion Energy, G-234, Department of Energy, Washington, DC 20545
53. D. Cohn, Massachusetts Institute of Technology, Cambridge, MA 02139
54. R. W. Conn, Fusion Technology Program, Nuclear Engineering Department, University of Wisconsin, Madison, WI 53706
55. CTR Library, c/o Alan F. Haught, United Technologies Research Laboratory, East Hartford, CT 06108
56. CTR Reading Room, c/o Allan N. Kaufman, Physics Department, University of California, Berkeley, CA 94720
57. Hatice Cullingford. Office of Fusion Energy, G-234, Department of Energy, Washington, DC 20545
58. J. Narl Davidson, School of Nuclear Engineering, Georgia Institute of Technology, Atlanta, GA 30332
59. Documentation S.I.G.N., Département de la Physique du Plasma et de la Fusion Controlée, Association EURATOM-CEA sur la Fusion, Centre d'Études Nucléaires, B.P. 85, Centre du TRI, 38041 Grenoble, Cedex, France
60. W. R. Ellis, Office of Fusion Energy, G-234, Department of Energy, Washington, DC 20545
61. G. A. Emmert, Nuclear Engineering Department, University of Wisconsin, Madison, WI 53706
62. Harold K. Forsen, Exxon Nuclear Co., Inc., 777 106th Avenue, N.E., C-000777, Bellevue, WA 98009

63. Harold P. Furth, Princeton Plasma Physics Laboratory, Princeton University, Forrestal Campus, P.O. Box 451, Princeton, NJ 08540
64. Roy W. Gould, California Institute of Technology, Mail Stop 116-81, Pasadena, CA 91125
65. Charles R. Head, Office of Fusion Energy, G-234, Department of Energy, Washington, DC 20545
66. Robert L. Hirsch, Exxon Research and Engineering, P.O. Box 101, Florham Park, NJ 07932
67. Raymond A. Huse, Manager, Research and Development, Public Service Gas and Electric Company, 80 Park Place, Newark, NJ 07101
68. T. Hsu, Office of Fusion Energy, G-234, Department of Energy, Washington, DC 20545
69. V. E. Ivanov, Physical-Technical Institute of the Ukranian Academy of Sciences, Sukhumi, U.S.S.R.
70. D. L. Jassby, Princeton Plasma Physics Laboratory, P.O. Box 451, Princeton, NJ 08540
71. A. Kadish, Office of Fusion Energy, G-234, Department of Energy, Washington, DC 20545
72. L. M. Kovrizhnikh, Lebedev Institute of Physics, Academy of Sciences of the U.S.S.R., Leninsky Prospect 53, Moscow, U.S.S.R.
73. Guy Laval, Groupe de Physique Théorique, Ecole Polytechnique, 91 Palaiseau, Paris, France
74. Library, Centre de Recherches en Physique des Plasma, 21 Avenue des Bains, 1007, Lausanne, Switzerland
75. Library, Culham Laboratory, United Kingdom, Atomic Energy Authority, Abingdon, Oxon, OX14 3DB, United Kingdom
76. Library, FOM-Institut voor Plasma — Fysica, Rijnhuizen, Jutphaas, Netherlands
77. Library, Institute for Plasma Physics, Nagoya University, Nagoya, Japan 464
78. Library, International Centre for Theoretical Physics, Trieste, Italy
79. Library, Laboratorio Gas Ionizzati, Frascati, Italy
80. Dsumber G. Lominadze, Academy of Sciences of the Georgian S.S.R., 8 Dzerzhinski St., 38004, Tbilisi, U.S.S.R.
81. Oscar P. Manley, Office of Fusion Energy, G-234, Department of Energy, Washington, DC 20545
82. D. G. McAlees, Exxon Nuclear Co., Inc., Research and Technology Laser Enrichment Department, 2955 George Washington Way, Richland, WA 99352
83. J. E. McCune, School of Engineering, Department of Aeronautics and Astronautics, Bldg. 37-391, Massachusetts Institute of Technology, Cambridge, MA 02139
84. Claude Mercier, Service du Theorie des Plasmas, Centre d'Études Nucléaires, Fontenay-aux-Roses (Seine), France
85. K. G. Moses, Office of Fusion Energy, G-234, Department of Energy, Washington, DC 20545
86. Michael Murphy, Office of Fusion Energy, G-234, Department of Energy, Washington, DC 20545

87. D. Pfirsch, Institute for Plasma Physics, 8046 Garching bei München, Federal Republic of Germany
88. Plasma Physics Group, Department of Engineering Physics, Australian National University, P.O. Box 4, Canberra A.C.T. 2600, Australia
89. Robert E. Price, Office of Fusion Energy, G-234, Department of Energy, Washington, DC 20545
90. A. Rogister, Institute for Plasma Physics, KFA, Postfach 1913, D-5170, Jülich 1, Federal Republic of Germany
91. W. Sadowski, Office of Fusion Energy, G-234, Department of Energy, Washington, DC 20545
92. V. D. Shafranov, I. V. Kurchatov Institute of Atomic Energy, 46 Ulitsa Kurchatova, P.O. Box 3402, Moscow, U.S.S.R.
93. Yu. S. Sigov, Institute of Applied Mathematics of the U.S.S.R. Academy of Sciences, Miuskaya, Sq. 4. Moscow A-47, U.S.S.R.
94. W. M. Stacey, Jr., School of Nuclear Engineering, Georgia Institute of Technology, Atlanta, GA 30332
95. L. D. Stewart, Princeton Plasma Physics Laboratory, P.O. Box 451, Princeton, NJ 08540
96. J. B. Taylor, Culham Laboratory, U.K. Atomic Energy, Authority, Abingdon, Oxon, OX14 3DB, United Kingdom
97. Thermonuclear Library, Japan Atomic Energy Research Institute, Tokai, Naka, Ibaraki, Japan
98. Francisco Verdaguer, Director, Division of Fusion, Junta de Energia Nuclear, Madrid 3, Spain
99. K. M. Zwilsky, Office of Fusion Energy, G-234, Department of Energy, Washington, DC 20545
100. Director, Research and Technical Support Division, Department of Energy, Oak Ridge Operations, P.O. Box E, Oak Ridge, TN 37830
101-335. Given distribution as shown in TID-4500, Magnetic Fusion Energy (Distribution Category UC-20a, d, and g: Plasma Systems, Fusion Systems, and Theoretical Plasma Physics)